

2-7-2013

## Optical Down-Conversion in Doped ZnSe:Tb<sup>3+</sup> Nanocrystals

Sandip Das

University of South Carolina - Columbia, dass@email.sc.edu

K. C. Mandal

University of South Carolina - Columbia, mandalk@enr.sc.edu

Follow this and additional works at: [https://scholarcommons.sc.edu/elct\\_facpub](https://scholarcommons.sc.edu/elct_facpub)



Part of the [Electrical and Electronics Commons](#), [Nanoscience and Nanotechnology Commons](#), and the [Optics Commons](#)

---

### Publication Info

Published in *Nanoscale*, Volume 5, Issue 3, 2013, pages 913-915.

© Nanoscale 2013, Royal Society of Chemistry

Das, S. K. & Mandal, K. C. (7 February 2013). Optical down-conversion in doped ZnSe:Tb<sup>3+</sup> nanocrystals. *Nanoscale*, 5(3), 913-915.

<http://dx.doi.org/10.1039/C2NR33243D>

This Article is brought to you by the Electrical Engineering, Department of at Scholar Commons. It has been accepted for inclusion in Faculty Publications by an authorized administrator of Scholar Commons. For more information, please contact [digres@mailbox.sc.edu](mailto:digres@mailbox.sc.edu).

## Optical down-conversion in doped ZnSe:Tb<sup>3+</sup> nanocrystals

Cite this: *Nanoscale*, 2013, 5, 913

Sandip Das and Krishna C. Mandal\*

Received 18th October 2012

Accepted 6th December 2012

DOI: 10.1039/c2nr33243d

[www.rsc.org/nanoscale](http://www.rsc.org/nanoscale)

Rare earth (RE) Tb<sup>3+</sup>-doped high quality ZnSe nanocrystals (NCs) were synthesized by a facile chemical hot-injection method. ZnSe:Tb<sup>3+</sup> nanocrystals exhibited broadband absorption below the first excitonic absorption peak. Photoluminescence spectra showed Tb<sup>3+</sup> emission lines in the visible spectral window at room temperature when excited by UV radiation below the band-edge of the host ZnSe nanocrystals. Our experimental results indicate optical down-conversion in these Tb<sup>3+</sup>-doped Zn-chalcogenide nanocrystals via energy migration from host ZnSe to the Tb<sup>3+</sup> dopant. The host-dopant energy transfer mechanism for this ZnSe:Tb<sup>3+</sup> nanocrystal system is correlated with the emission spectra.

Doped bulk and 2-dimensional semiconductors have led to today's technological advancements in the design of state-of-the-art electronic and optoelectronic devices. Intentionally introducing the dopant atoms into a semiconductor lattice allows tuning of the properties of the host semiconductor material. In order to achieve such control over the properties of nanoscale devices, recently researchers have attempted to realize controlled doping of nanoscale semiconductor materials. Semiconductor nanocrystals (SNCs) show unique tunable optoelectronic properties arising from the quantized energy levels in a nanoscale regime, which can be further exploited to its maximal extent by doping these materials.<sup>1,2</sup> Such doped nanomaterials find diverse applications in emerging fields, such as, nano-optoelectronics, quantum computing and bio-imaging. Recently, Mn<sup>2+</sup>-doped nanocrystals have been shown to have enhanced photoluminescence efficiency with tunable optical and magnetic properties.<sup>3-5</sup> However, only a few dopants on limited host SNCs have been studied so far. It is important to study the effects of new dopants in different host nanocrystals for the development of future generation functional nanomaterials. Doping of rare earth (RE) lanthanides to various

hosts has been investigated for applications in Mid-IR Lasers<sup>6-8</sup> and optical down-conversion.<sup>9-17</sup> Particularly, Tb<sup>3+</sup> and Yb<sup>3+</sup> have attracted much attention due to their quantum cutting capability resulting in visible and near-infrared emission which can lead to enhanced solar spectral matching and improved solar cell efficiency. Most of these investigations were focused on introducing rare earth lanthanides in complex oxides/phosphors,<sup>9,10</sup> glass/ceramics<sup>11</sup> or in fluoride based hosts.<sup>12,13</sup> However, due to the competing non-radiative relaxation mechanism and poor broadband absorption of these traditional oxides, ceramics or phosphor based hosts, their application as a down-conversion material is limited. Energy transfer to dopants can be significantly enhanced in SNCs due to the high degree of spatial confinement and the competing surface recombination processes can be mitigated.<sup>14</sup>

Recently, we have demonstrated optical down-conversion in Tb<sup>3+</sup> and Yb<sup>3+</sup>-doped CdS nanocrystals.<sup>15</sup> However, toxicity of Cd is a potential hindrance to the wide scale application of CdS-based down-converters. Recently, doped ZnSe nanocrystals have been investigated by several groups and have been reported to show efficient color-tunability and tunable impurity emissions.<sup>18,19</sup> Here, for the first time we report the synthesis of Tb<sup>3+</sup>-doped ZnSe nanocrystals and their structural and optical properties showing down-conversion in ZnSe:Tb<sup>3+</sup>. ZnSe possess extremely low toxicity compared to CdS and it has a bulk bandgap of ~2.70 eV at 300 K; which makes it a suitable candidate for absorbing near UV radiation and harvesting high energy photons.

Host ZnSe nanocrystals were synthesized by a hot injection method using ZnO as a Zn precursor and elemental Se powder as a Se source. Terbium acetate was used as the source for Tb<sup>3+</sup>-doping. In a typical synthesis, 2.5 mmol of ZnO, 0.125 mmol of terbium acetate (5 mol% of Zn precursor), 30 mmol of oleic acid and 4 mmol of hexadecylamine were heated to 320 °C in a 50 ml three-necked flask under argon ambient. Se powder dissolved in tri-*n*-octylphosphine (TOP) (197.4 mg Se powder dissolved in 1.5 ml of TOP) was then quickly injected into the Zn precursor solution and the nanocrystals were grown at 280 °C (±2 °C). The

Department of Electrical Engineering, University of South Carolina, Columbia, South Carolina, 29208, USA. E-mail: mandalk@cec.sc.edu; Fax: +1 803 777 8045; Tel: +1 803 777 2722

flask was removed from the heating mantle to seize the reaction after desired growth time. Doped ZnSe nanocrystals of different sizes were synthesized by controlling the growth time. The as-grown ZnSe nanocrystals were purified by successive precipitation and decantation cycles for at least two times using acetone and hexanes following the standard literature method.<sup>5</sup> Finally, the purified nanocrystals were suspended in hexanes for further characterization.

Structural characterization of the doped ZnSe nanocrystals was carried out using a Rigaku D/Max 2100 powder X-ray diffractometer equipped with a diffracted beam graphite monochromator with a  $\text{CuK}\alpha$  source ( $\lambda = 1.5418 \text{ \AA}$ ) and the resulting diffraction pattern is shown in Fig. 1. XRD peaks were indexed with reference to zinc blende (JCPDS card # 01-071-5977) and wurtzite (JCPDS card # 01-089-2940) phases of ZnSe single crystal XRD characteristic lines represented by vertical straight lines in the figure. The nanocrystals showed the best match to the zinc blende phase (cubic). However, coexistence of a wurtzite phase (hexagonal) cannot be discarded. Broadened characteristic peaks indicate the nanoscale domain of the crystallites. The most dominant peaks corresponding to (111), (220), (311), (331), (420), (422) and (511) planes were identified and found to be in good agreement with the literature.<sup>20</sup>

Optical characterizations were carried out by UV-Vis absorption spectroscopy and photoluminescence (PL) spectroscopy using a Perkin-Elmer Lambda 750 spectrophotometer and a Horiba Jobin-Yvon Fluorolog 3 spectrofluorometer respectively. UV-Vis absorbance spectra of ZnSe:Tb<sup>3+</sup> SNCs showing the evolution of the first excitonic peak with increasing growth time are shown in Fig. 2. The first order excitonic absorption peak is red shifted with increased growth time indicating the increased size of the nanocrystals. Sharp absorption peaks are indicative of nearly monodisperse nanocrystals with narrow size distribution.

Fig. 3(a) shows the photoluminescence (PL) spectra of Tb<sup>3+</sup>-doped ZnSe nanocrystals for 5 mol% Tb<sup>3+</sup>-doped ZnSe

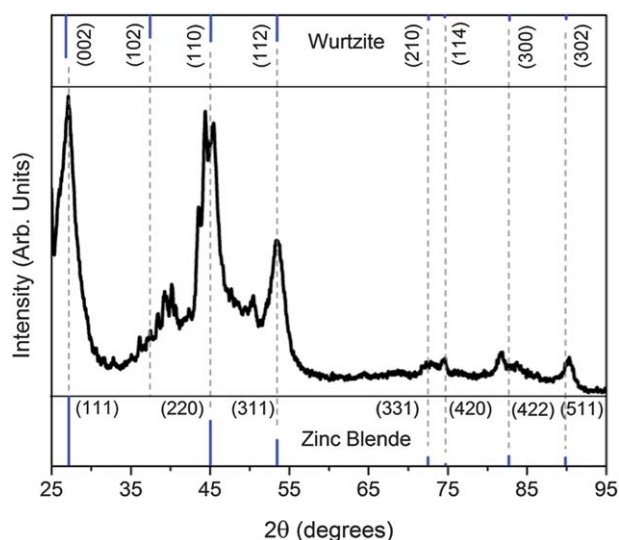


Fig. 1 XRD pattern of Tb<sup>3+</sup>-doped ZnSe nanocrystals.

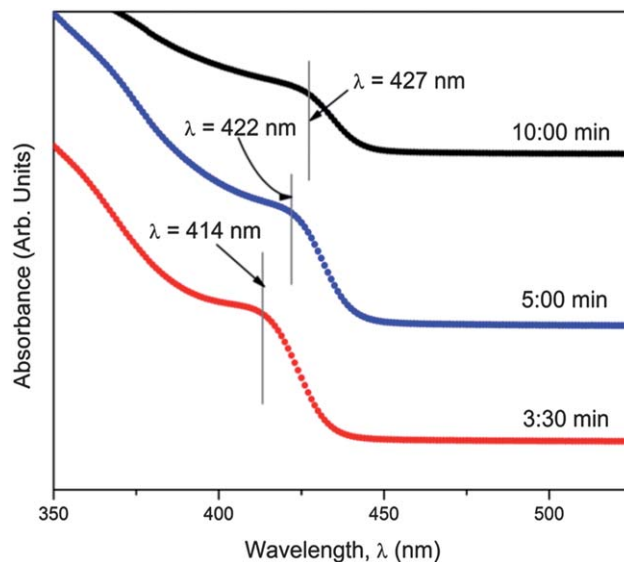


Fig. 2 Absorbance spectra showing the evolution of the first excitonic peak of the doped-ZnSe nanocrystals with increasing growth time.

nanocrystals. In Fig. 3(b), the emission spectra of corresponding undoped ZnSe SNCs are shown. PL spectra were obtained at 350 nm excitation wavelength, well below the band-edge of host ZnSe nanocrystals. For doped SNCs, pronounced emission lines of terbium  $^5\text{D}_4 \rightarrow ^7\text{F}_j$  ( $j = 6, 5, 4, 3$ ) transitions ( $^5\text{D}_4 \rightarrow ^7\text{F}_6$  at 484 nm,  $^5\text{D}_4 \rightarrow ^7\text{F}_5$  at 543 nm,  $^5\text{D}_4 \rightarrow ^7\text{F}_4$  at 584 nm and  $^5\text{D}_4 \rightarrow ^7\text{F}_3$  at 623 nm) in the visible window are observed. The most dominant Tb<sup>3+</sup> emission appearing at 543 nm is attributed to the  $^5\text{D}_4 \rightarrow ^7\text{F}_5$  transition emitting green light.

The broad ZnSe peak in the background is due to the surface defects. Introducing a core-shell structure to passivate these doped nanocrystals with a higher bandgap material (such as ZnS) can further improve the emission properties. This downconversion property can be exploited and retrofitted to get better solar spectral matching to enhance photo-conversion efficiency of all existing solar cells. Shell passivation and RE-doped core-shell nano-structures are presently under investigation.

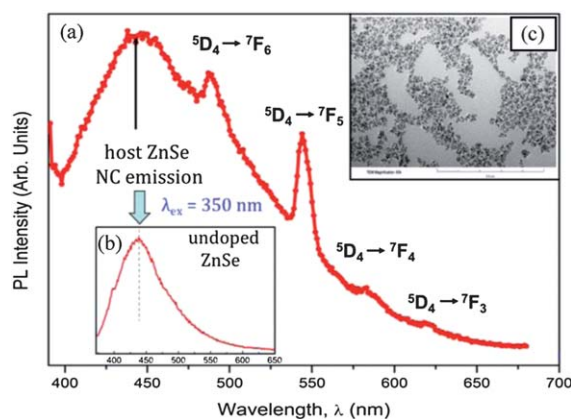


Fig. 3 PL spectra of (a) Tb<sup>3+</sup>-doped ZnSe SNCs, (b) undoped ZnSe SNCs and (c) TEM image of the doped ZnSe SNCs at 60 K magnification.

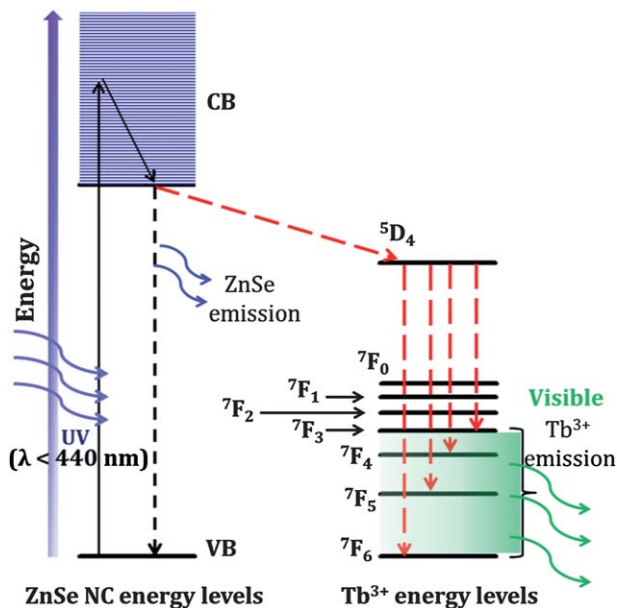


Fig. 4 Energy levels and down-conversion in  $\text{Tb}^{3+}$ -doped ZnSe nanocrystals.

According to the Dieke diagram,<sup>21</sup> the energy levels of the ZnSe host and trivalent  $\text{Tb}^{3+}$ -ion are shown in Fig. 4 and the host-dopant energy transfer process is shown schematically. Host ZnSe acts as the energy receptor antenna and a donor to the  $\text{Tb}^{3+}$ . The  $^5\text{D}_4$  excited state of the  $\text{Tb}^{3+}$  ion is situated approximately at  $20\,000\text{ cm}^{-1}$  above the  $^7\text{F}_6$  ground state, which receives the energy from the ZnSe host and relaxes to four different lower energy states ( $^7\text{F}_3$ – $^7\text{F}_6$ ) corresponding to visible emissions at 484 nm, 543 nm, 584 nm and 623 nm respectively. Our result clearly demonstrates that  $\text{RE}^{3+}$ -doped ZnSe nanocrystals can serve as a potential down-conversion material, alternative to  $\text{RE}^{3+}$ -doped cadmium based toxic nanocrystals.

## Conclusions

We have successfully doped ZnSe host nanocrystals with rare earth (RE) terbium ( $\text{Tb}^{3+}$ ) ions and demonstrated down-conversion of high energy UV photons using this novel  $\text{RE}^{3+}$ -doped nanocrystals. The synthesized ZnSe host nanocrystals were found to have a narrow size distribution, confirmed by sharp excitonic peaks in UV-Vis absorbance spectra. The  $\text{RE}^{3+}$ -doped nanocrystals showed emissions in the visible region due to  $\text{Tb}^{3+}$  transitions when excited by high energy photons below the band edge of host ZnSe nanocrystals. We conclude that these novel  $\text{RE}^{3+}$ -doped cadmium free, non-toxic, environment friendly nanocrystals have the potential to be employed as a down-conversion material for harvesting higher energy UV photons resulting in enhanced solar cell efficiency.

## Acknowledgements

The authors acknowledge the financial support from DARPA, Grant Number # N66001-10-1-4031. The authors are also thankful to Dr MVS Chandrashekhar for providing UV-Vis and PL measurement facilities.

## Notes and references

- D. J. Norris, A. L. Efros and S. C. Erwin, *Science*, 2008, **319**, 1776–1779.
- S. C. Erwin, L. Zu, M. I. Haftel, A. L. Efros, T. A. Kennedy and D. J. Norris, *Nature*, 2005, **436**, 91–94.
- N. Pradhan, D. Goorskey, J. Thessing and X. Peng, *J. Am. Chem. Soc.*, 2005, **127**, 17586–17587.
- H. Yang and P. H. Holloway, *Appl. Phys. Lett.*, 2003, **82**, 1965.
- R. Zeng, M. Rutherford, R. Xie, B. Zou and X. Peng, *Chem. Mater.*, 2010, **22**, 2107–2113.
- K. C. Mandal, S. H. Kang, M. Choi and R. D. Rauh, *Int. J. High Speed Electron. Syst.*, 2008, **18**, 735–745.
- K. Rademaker, W. F. Krupke, R. H. Page, S. A. Payne, K. Peterman, G. Huber, A. P. Yeliseyev, L. I. Isaenko, U. N. Roy, A. Burger, K. C. Mandal and K. Nitsch, *J. Opt. Soc. Am. B*, 2004, **21**, 2117–2129.
- U. N. Roy, R. H. Hawrami, Y. Cui, S. Morgan, A. Burger, K. C. Mandal, C. C. Noblitt, S. A. Speakman, K. Rademaker and S. A. Payne, *Appl. Phys. Lett.*, 2005, **86**, 151911.
- X. Y. Huang, D. C. Yu and Q. Y. Zhang, *J. Appl. Phys.*, 2009, **106**, 113521–113526.
- Q. Zhang, J. Wang, G. Zhang and Q. Su, *J. Mater. Chem.*, 2009, **19**, 7088–7092.
- S. Ye, B. Zhu, J. X. Chen, J. Luo and J. R. Qiu, *Appl. Phys. Lett.*, 2008, **92**, 141112.
- Z. L. Wang, Z. W. Quan, P. Y. Jia, C. K. Lin, Y. Luo, Y. Chen, J. Fang, W. Zhou, C. J. O'Connor and J. Lin, *Chem. Mater.*, 2006, **18**, 2030–2037.
- L. Wang and Y. Li, *Chem. Mater.*, 2007, **19**, 727–734.
- R. N. Bhargava, *J. Lumin.*, 1996, **70**, 85–94.
- S. Das and K. C. Mandal, *Mater. Lett.*, 2012, **66**, 46–49.
- W. Ren, G. Tian, L. Zhou, W. Yin, L. Yan, S. Jin, Y. Zu, S. Li, Z. Gu and Y. Zhao, *Nanoscale*, 2012, **4**, 3754–3760.
- R. Liu, D. Tu, Y. Liu, H. Zhu, R. Li, W. Zheng, E. Ma and X. Chen, *Nanoscale*, 2012, **4**, 4485–4491.
- N. Pradhan and X. Peng, *J. Am. Chem. Soc.*, 2007, **129**, 3339–3347.
- N. Pradhan, D. Goorskey, J. Thessing and X. Peng, *J. Am. Chem. Soc.*, 2005, **127**, 17586–17587.
- P. D. Cozzoli, L. Manna, M. L. Curri, S. Kudera, C. Giannini, M. Striccoli and A. Agostiano, *Chem. Mater.*, 2005, **17**, 1296–1306.
- G. H. Dieke, *Spectra and energy levels of rare earth ions in crystals*, Interscience Publishers, New York, 1968.